Optimizing Grid Regulation With Gravity Storage Systems: A Comparative Analysis With Different Motor Inertias

Preprint

Shubham Sundeep,[1] Latha Sethuraman,[1] Dayo Akindipe,[1] Lee Jay Fingersh,[1] Zach Wenrick,[2] and Aaron Munoz[2]

1 National Renewable Energy Laboratory
2 Renewell Energy

Presented at IEEE Energy Conversion Congress & Expo
Phoenix, Arizona
October 20–24, 2024

NREL is a national laboratory of the U.S. Department of Energy
Office of Energy Efficiency & Renewable Energy
Operated by the Alliance for Sustainable Energy, LLC

This report is available at no cost from the National Renewable Energy Laboratory (NREL) at www.nrel.gov/publications.

Contract No. DE-AC36-08GO28308

Conference Paper
NREL/CP-5000-90657
October 2024

Optimizing Grid Regulation With Gravity Storage Systems: A Comparative Analysis With Different Motor Inertias

Preprint

Shubham Sundeep,[1] Latha Sethuraman,[1] Dayo Akindipe,[1] Lee Jay Fingersh,[1] Zach Wenrick,[2] and Aaron Munoz[2]

1 National Renewable Energy Laboratory
2 Renewell Energy

Suggested Citation
Sundeep, Shubham, Latha Sethuraman, Dayo Akindipe, Lee Jay Fingersh, Zach Wenrick, and Aaron Munoz. 2024. *Optimizing Grid Regulation With Gravity Storage Systems: A Comparative Analysis With Different Motor Inertias: Preprint*. Golden, CO: National Renewable Energy Laboratory. NREL/CP-5000-90657.
https://www.nrel.gov/docs/fy25osti/90657.pdf.

NREL is a national laboratory of the U.S. Department of Energy
Office of Energy Efficiency & Renewable Energy
Operated by the Alliance for Sustainable Energy, LLC

This report is available at no cost from the National Renewable Energy Laboratory (NREL) at www.nrel.gov/publications.

Contract No. DE-AC36-08GO28308

Conference Paper
NREL/CP-5000-90657
October 2024

National Renewable Energy Laboratory
15013 Denver West Parkway
Golden, CO 80401
303-275-3000 • www.nrel.gov

NOTICE

This work was authored in part by the National Renewable Energy Laboratory, operated by Alliance for Sustainable Energy, LLC, for the U.S. Department of Energy (DOE) under Contract No. DE-AC36-08GO28308. Funding provided by U.S. Department of Energy Advanced Research Projects Agency-Energy. The views expressed herein do not necessarily represent the views of the DOE or the U.S. Government. The U.S. Government retains and the publisher, by accepting the article for publication, acknowledges that the U.S. Government retains a nonexclusive, paid-up, irrevocable, worldwide license to publish or reproduce the published form of this work, or allow others to do so, for U.S. Government purposes.

Cover Photos by Dennis Schroeder: (clockwise, left to right) NREL 51934, NREL 45897, NREL 42160, NREL 45891, NREL 48097, NREL 46526.

Optimizing Grid Regulation With Gravity Storage Systems: A Comparative Analysis With Different Motor Inertias

Shubham Sundeep
National Wind Technology Center
National Renewable Energy Laboratory,
Golden, CO, USA
shubham.sundeep@nrel.gov

Latha Sethuraman
National Wind Technology Center
National Renewable Energy Laboratory,
Golden, CO, USA
latha.sethuraman@nrel.gov

Dayo Akindipe
Energy Conversion and Storage Systems
National Renewable Energy Laboratory,
Golden CO, USA
dayo.akindipe@nrel.gov

Lee Jay Fingersh
National Wind Technology Center
National Renewable Energy Laboratory,
Golden, CO, USA
lee.fingersh@nrel.gov

Zach Wenrick
Renewell Energy
Bakerfield, CA, USA
zach@renewellenergy.com

Aaron Munoz
Renewell Energy
Bakerfield, CA, USA
aaron@renewellenergy.com

***Abstract*—The integration of renewable energy sources into power grids necessitates solutions for grid support and stability during fluctuations in electricity generation and demand. Gravity energy storage systems (GESS) are emerging as a promising technology for managing the balance between energy supply and demand. However, their capacity to optimize energy flow and offer voltage and frequency regulation amid imbalances in generation and demand is less reported. This paper investigates the control of GESS for optimizing energy flow during voltage and frequency regulation. The study evaluates the regulation capabilities of GESS with different motor inertias during a Texas grid event: one with a high-speed, low-inertia motor and another with a low-speed, high-inertia motor. Results indicate that both GESS scenarios provide fast frequency response by converting potential energy into kinetic energy and vice versa, with a response time of 1.5 s from the frequency variation. This aligns with grid requirements for primary frequency response from traditional synchronous generators and motors with large inertia. Furthermore, a GESS based on a high-inertia motor may be able to operate over a broader range of frequency variations, whereas a low-inertia system may be limited by thermal constraints of the motor.**

Keywords— Frequency regulation, Gravity energy storage system, Grid stability, Voltage regulation.

I. INTRODUCTION

The integration of renewable energy sources such as solar and wind to existing grids causes frequent imbalances in generation and demand due to their intermittent availability. Additionally, the increased electrification of transportation and industrial sectors could lead to load variations, further destabilizing the supply-demand equilibrium. These imbalances affect grid stability, causing fluctuations in frequency and voltage for long durations. According to the Electric Reliability Council of Texas (ERCOT) grid codes [1-2], power generation sources are expected to respond within 14–16 s of a grid imbalance [1-2]. To address these issues, several strategies are employed: (1) increasing generation flexibility to meet maximum load demand [3-4]; (2) planning interconnections between generation sources with frequency stability as a key constraint [5-6]; and (3) integrating energy storage systems (ESS) with the grid [7-18]. Similarly, the widespread use of the renewable energy sources on the grid causes fluctuations in reactive power, resulting in voltage fluctuations known as sag and swell. This is revolved using a flexible AC transmission system (FACTS) [19], which consists of power electronic converters. The first two strategies rely on the mechanical response of conventional governors in large synchronous generators to change their speed of operation, also called "inertial response" to a grid instability, the typical response times of which are within 5 to 30 s. They have slower ramp-up and ramp-down time, making them less suitable for a quick response to sudden changes in grid condition. Quick response time is required to reduce the grid frequency and voltage deviation, which results in load shedding. For instance, according to ERCOT [20], a generation loss of 2.75 GW takes 0.413 s for frequency to drop from 59.7 Hz to 59.3 Hz, and frequency lower than 59.7 Hz triggers underfrequency relay that would lead to load shedding within 20 to 30 cycles. Therefore, the primary frequency response should be less than 0.5 s to arrest frequency and avoid involuntary load shedding.

However, ESS technologies such as flywheel energy storage systems (FESS) [7-8], battery energy storage systems (BESS) [9-11], virtual inertia [11], and mechanical energy storage systems [14-18]are power electronic converter-based resources with fast response times, making them highly effective for voltage and frequency regulation and grid stability by monitoring the grid frequency and adjusting the power output of the storage system (charging or discharging). The converters play a vital role in power transfer between the grid and the ESS, especially during grid instability. However, it does not contribute to the system inertia. While FESS and BESS offer fast response times and high efficiency, they are limited in their storage capacity and are capital-intensive. Although the FESS responds in less than 4 ms [16], its discharge time is limited to 15 minutes. On the other hand, the typical response time of the BESS is less than 40 ms [16], but it degrades with each charge-discharge cycle and suffers from self-discharge [11]. Furthermore, the DC-link capacitors shows great promise in emulating virtual inertia that mimics inertial response as energy stored in the capacitor, albeit with complex control [11]. The mechanical energy storage systems like pumped storage hydropower [14-16] and gravity energy storage systems (GESS) [17-18] use rotating masses for providing inertial response with efficient control and degradation-free support. Rapid response to any contingency event is possible in these systems because the rotating masses are decoupled from the grid via the DC-link and a converter system. However, pumped storage hydropower in particular faces challenges, including high up-front capital costs, geographical constraints necessitating specific topographical

features, and potential environmental impacts like habitat disruption and water use [16]. On the other hand, because GESS is a relatively new technology, its frequency regulation capabilities have been less reported [21]. Tong et al. [22] discussed the operation of a 1 MW GESS connected to other energy sources within a microgrid. The system utilized a suspended mass through a winch-rope system and was shown to provide unidirectional frequency regulation (during the charging phase when the frequency is rising and during the discharging phase when the frequency is falling). However, specific details on the controls during a contingency were not available to assess their directional response, the importance of storage capacity, and system inertia. Importantly, traditional GESS such as those by Gravitricity [21] use high-speed motors with a lower inertia when compared to traditional synchronous machines. As a result, their fast frequency regulation capabilities will be solely reliant on the control mechanism, and it is unclear what response times are achievable. Further, GESS can also address voltage variation through reactive power compensation, also known as voltage regulation, without the need for additional converters. To better understand the control and voltage and frequency regulation capabilities, including directional response, the role of storage capacity, and inertia of the drive system, we developed and simulated a MATLAB-based model of one such GESS, with different motor inertias.

The GESS under study is a 36 kWh system designed by Renewell Energy [23] that repurposes an idle oil well for energy storage to meet energy needs in areas with high grid fluctuations. The frequency regulation capabilities of such a system are demonstrated for a frequency drop event in the Texas grid during the February 2021 blackout [24]. The results show that the response of the GESS depends on the conversion of its stored potential energy into kinetic energy by accelerating and decelerating its rotating mass.

The paper is structured as follows: Section II outlines the challenges in frequency regulation using conventional sources and the potential advantages of integrating a GESS. Section III describes the GESS, and Section IV illustrates the control algorithm used for providing frequency and voltage regulation. Section V presents the results showcasing the frequency and voltage regulation capability of the GESS during both charging and discharging modes. Additionally, Section V compares the performance of the two GESS of different rotor inertia during the frequency drop in the Texas grid in February 2021. Section VI provides the conclusion.

II. Frequency Regulation Using Conventional Sources and a GESS

In traditional power systems, the kinetic energy stored in the rotating masses of the synchronous generators and motor loads synchronized to the system is used to counteract power imbalances, thereby resisting any changes in system frequency. This resistance to frequency variation is referred to as inertia response, which depends on the inertia constant of the system. The inertia constant (H_{sys}) is mathematically expressed as the ratio between the total kinetic energy (E_k) of all generating sources and loads connected to the grid and the MVA rating of the base system (S_{base}) [20];

$$H_{sys} = \frac{E_k}{S_{base}} = \frac{\omega^2}{2S_{base}} \sum_{i=1}^{n} J_i \quad (1)$$

where, J_i is the moment of inertia of the i^{th} generator, n is the total number of generators, and ω is the angular speed of the generators. The overall inertia of the system is significantly influenced by both the quantity and size of the online generators and motor loads that are synchronized with it. Generally, the inertial response of the motor loads is lumped into a load damping constant. During a power imbalance event, such as when load demand exceeds generation, a rise in frequency occurs. The kinetic energy stored in the large synchronous generators is used to meet the generation deficit. The speed governors regulate the speed to stabilize the system frequency. However, the typical response time of the speed governors is 5 to 30 s due to the high inertia of the synchronous generators. The initial rate of change of frequency (ROCOF) prior to any inertia response depends on the power imbalance (ΔP) and system inertia (H_{sys}) as [20]

$$ROCOF = \frac{f_0}{2H_{sys}} \frac{\Delta P}{S_{base}} = \frac{f_0 \Delta P}{2E_k} \quad (2)$$

It is important to note that greater power imbalances or lower system inertia result in a higher ROCOF, which causes more frequent frequency variations. As the penetration of renewable energy sources in the grid is increasing, system inertia is decreasing. This is because renewable energy sources are coupled to the grid through power electronic converters, which do not possess inertia. For example, the inertia constant of different generation types in ERCOT listed in Table I [20] shows that nonsynchronous, inverter-based resources like solar and wind generation do not contribute to the system inertia. The system inertia determines the initial ROCOF. When system inertia is low, the Rate of Change of Frequency (ROCOF) following an imbalance event will be greater. A high ROCOF doesn't allow enough time for synchronous response mechanisms to activate and stabilize the frequency before it drops below the underfrequency load shedding threshold. As a result, this could lead to unintended disconnection of loads. Recently, grid-forming inverter-based controls have been used to integrate renewable energy sources with the grid, which uses a DC-link capacitor to emulate inertia. However, it involves complex controls [11].

TABLE I. Inertia Constant and Base MVA of Different Types of Resources in ERCOT [19].

Source Type	Base MVA	Inertia constant (s)
Nuclear	1410-1504	3.8-4.34
Coal	194-1120	2.9-4.5
Cumbustion turbine	7-235	1-12.5
Gas steam	14-887	1-5.4
Combined cycle	25-1433	1-1.9
Hydro	9-36	2-3
Reciprocating engine	10-70	1.1-2.1
Wind	-	0
Solar PV	-	0

Integrating a GESS can mitigate these issues by injecting or withdrawing power, which reduces the ROCOF of the system and helps to avoid a lower frequency nadir. Thus, despite having low inertias, GESS can be controlled to provide fast frequency response. For instance, when the GESS is integrated to the power system, the ROCOF of the system is expressed as [20]

$$ROCOF = \frac{f_0}{2H_{sys}} \frac{(\Delta P - \Delta P_{GESS})}{S_{base}} = \frac{f_0(\Delta P - \Delta P_{GESS})}{2E_k} \quad (3)$$

where ΔP_{GESS} is the power contributed by the GESS. Deploying the GESS can arrest any frequency decay and avoid involuntary load disconnection.

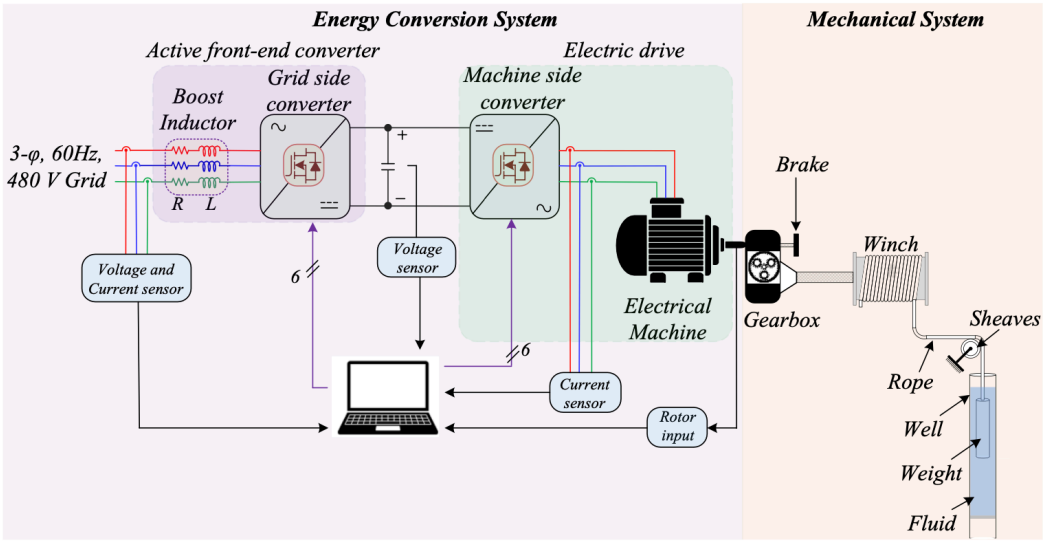

Fig. 1. A schematic diagram of the gravity energy storage system under study.

III. Operation and Control of the Gravity Energy Storage System

For this study we modeled and simulated a GESS designed by Renewell Energy [23] that repurposes an idle oil well as an environment for a cylindrical weight to move, as illustrated in Fig. 1. We studied its frequency regulation capabilities when connected to a three-phase, 480 V, 60 Hz grid with a low-inertia or a high-inertia permanent magnet synchronous machine in the MATLAB/Simulink environment. The low-inertia machine is a three-phase, 460 V, 1800 rpm, 100 hp permanent magnet synchronous machine manufactured by Baldor Reliance Motors [25] with a rotor inertia of 0.493 kg m^2. The electrical system comprises a three-phase two-level front-end converter connected to a three-phase two-level machine-side converter through a DC-link. The front-end converter is regulated to maintain a constant DC-link voltage while the machine-side converter is controlled to deliver the required load torque by the electrical machine.

This system is engineered to efficiently store and discharge energy by using the gravitational potential energy of the cylindrical weight moving inside a fluid-filled well with the help of a bidirectional power converter. During charging, the power converter draws power from grid to lift the weight using a winch and wire rope system. The resultant mechanical energy is then stored as gravitational potential energy in the weight. During the discharging process, the mechanical system descends the weight to release the potential energy stored within it. The potential energy is then converted into electrical energy by the energy conversion system and supplied to the grid. For a given mass (m) of the cylinder, the energy capacity (E) of the well is defined as [17]

$$E(kWh) = 2.77 \times 10^{-7} \times mgh \qquad (4)$$

where g is the acceleration due to gravity, and h is the depth available for traversing. In this study, a well with a depth of 1527.66 m, filled with a fluid of density 965.96 kg m^{-3}, and a cylindrical object weighing 15.34 metric tons and length 327.66 m are selected. The cylinder is suspended through a steel rope, which is wound on a cylindrical winch on the other end. The usable depth for energy storage, defined as the difference between the well depth and the length of the cylindrical object, is 1200 m. The electrical machine shaft is connected to the input shaft of the gearbox to reduce its speed from 1800 rpm to 11.44 rpm. Taking into account the buoyant force exerted by the fluid, the energy capacity of the system is determined to be 36 kWh. It is important to note that the energy capacity relies on factors such as the mass of the object and the depth available for traversing, which limits the energy provided during frequency regulation.

The energy conversion system of the GESS comprises an active front-end converter feeding an electric drive. The active front-end converter converts the AC grid voltage into DC voltage through a reactor and a grid-side voltage source converter. A DC capacitor is connected across the DC terminal for a rigid bus voltage to ensure DC voltage ripple within its limits [26]. Moreover, the converter is controlled through field-oriented control to ensure bidirectional power flow and controlled power factor. The bidirectional power flow is essential, as it entails the transfer of power between the grid and the DC-link during frequency regulation. Additionally, the control over the power factor allows for reactive power compensation to the grid during a voltage sag or swell event.

At the output of the front-end converter, an electric drive is connected that comprises a machine-side converter and an electrical motor. The converter is controlled using rotor field-oriented control to transfer power between the DC link and the mechanical system. The converter adjusts the speed of the motor to regulate the power drawn from and fed back to the grid depending on the position of the weight inside the well. The speed, position of the weight inside the well, and torque of the machine are respectively regulated using dedicated speed, position, and current controllers [26]. A frequency regulator controller algorithm monitors the grid frequency and adjusts the active power output of the storage system (charging or discharging) by adjusting the speed of the machine as necessary.

IV. Frequency and Voltage Regulation Control of the GESS

A typical frequency-watt curve [1] is illustrated in Fig. 2. It shows the anticipated variation of output active power of the GESS in response to the changes in the grid frequency. The deadband region centered around the nominal frequency depicts the scenario where the controller does not adjust the active power in response to the variation in frequency. This

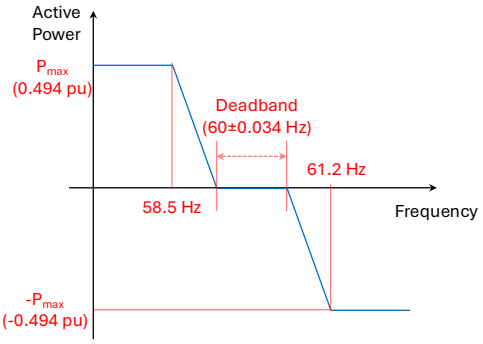

Fig. 2. Frequency-watt curve used for active power compensation during frequency regulation.

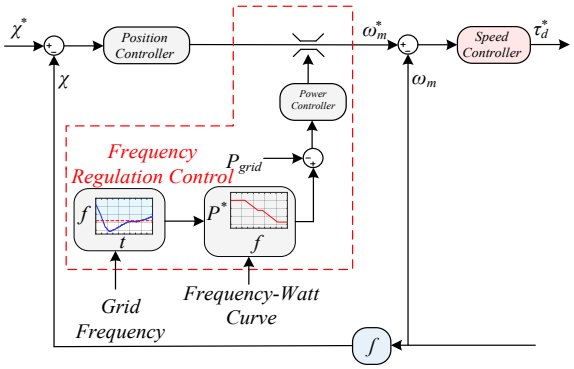

Fig. 3. A schematic diagram illustrating frequency regulation control, which adjusts the machine speed to provide active power compensation.

relieves the system from continuous adjustment and reduces wear and tear. When the frequency drops beyond the deadband region, the frequency regulation controller should act quickly to increase the power injected into the grid. If the frequency falls below 58.50 Hz, the controller should maintain this increased active power at 49.4% of the GESS's power rating. Conversely, when the frequency rises beyond the deadband region, the controller decreases the active power injected into the grid by adjusting the machine speed. If the frequency exceeds 61.20 Hz, the controller reduces the power to 49.4% of the GESS's rated power.

The frequency regulation control (as depicted in Fig. 3) uses this curve to regulate the active power by adjusting the speed of the electrical machine. The controller adjusts the speed by limiting the output of the position controller. The position controller regulates the position of the cylinder inside the well. The output of the position controller is the reference speed (ω^*), which is compared with the actual speed of the machine (ω) and fed to the speed controller. Based on the speed error, the speed controller generates the reference torque (τ^*). The reference torque is further used, as in field-oriented control, to control the electrical machine.

During frequency regulation, the active power compensation is provided by using the kinetic energy of the rotating mass. For instance, in grids with significant renewable energy penetration, a generation loss can cause the grid frequency to drop. The ROCOF, governed by system inertia as per (2), increases with lower inertia. Injecting active power into the grid restores the frequency, whereas excess active power is absorbed by converting stored potential energy in the GESS into kinetic energy.

Fig. 4. depicts a volt-VAR curve [1], which describes anticipated variation of reactive power output of the GESS in

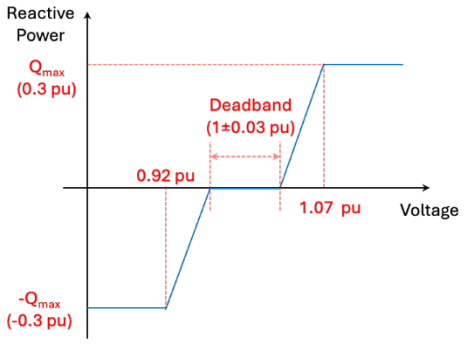

Fig. 4. Volt-VAR curve used for reactive power compensation during volatge regulation.

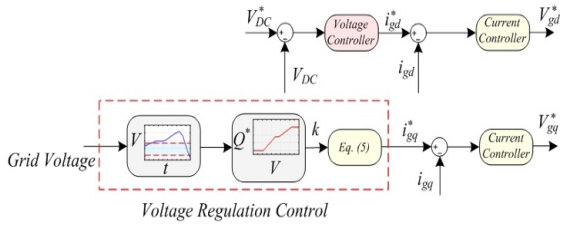

Fig. 5. A schematic diagram illustrating volatge regulation control, which adjusts the reactive component of the grid current to provide reactive power compensation.

response to the changes in the grid voltage. During voltage regulation, reactive power compensation is provided by adjusting the reactive component of the grid current (q-axis current) of the front-end converter.

Therefore, the voltage regulation can be realized without a change in the control of the machine-side converter. Similar to the frequency-watt curve, the volt-VAR curve consists of a deadband region centered around the nominal voltage where the controller does not adjust the reactive power in response to the variation in voltage. Therefore, the q-axis grid current reference, as illustrated in Fig. 5, is set to zero.

When the voltage increases above 1.03 p.u., the reactive power is injected to the grid by adjusting the q-axis current reference using (5) and the volt-VAR curve:

$$i_q^* = k\frac{VA\ Rating}{Rated\ Voltage} \tag{5}$$

where k is the reactive power compensation in p.u., derived from the volt-VAR curve. A similar compensation is provided in case of a decrease in the voltage, wherein the excess reactive power is absorbed from the grid.

V. Results

A. Performance of a Gravity Energy Storage System During Frequency Regulation

Fig. 6 (a) shows a contingency event when a generation deficit at the grid happens at instant "A" is accompanied by a frequency dip to below 59.6 Hz at instant "B." This lasts for a duration of 7 s. We simulated this scenario when the system is charged to 96% of its capacity and is either charging or discharging. Prior to instant "A," the GESS is operating in constant power mode. The grid frequency can be restored by effectively controlling the stored kinetic energy in the GESS to inject or absorb power from the grid depending on whether it is discharging or charging.

For the purpose of inertia support, the GESS primarily

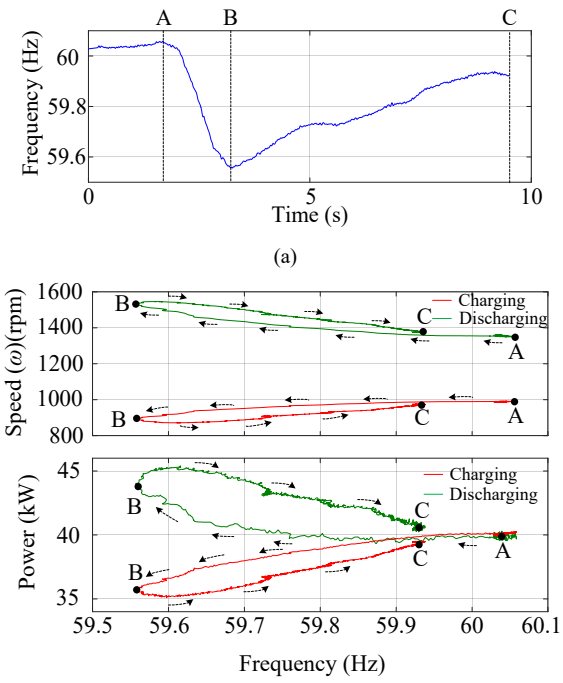

Fig. 6. Diagram of the frequency regulation control to control the grid power by adjusting the speed of the machine.

relies on the conversion of its stored potential energy into kinetic energy (E_k) by accelerating or decelerating the rotational speed (ω) of its rotating masses, which is expressed mathematically as [21]

$$E_k = \frac{1}{2} J_{eq} \omega^2 \tag{6}$$

where, J_{eq} is the equivalent moment of inertia of the rotating masses consisting of two main components: one representing the moment of inertia of the connected motor, winch, and sheave shaft, and the other representing the equivalent moment of inertia of the suspended mass's kinetic energy.

Figure 6 (b) illustrates the change in motor speed and grid active power during a frequency drop during charging and discharging. During discharging, as the grid frequency decreases from point "A" to point "B," the speed of the machine increases by leveraging the stored potential energy that is converted to its kinetic energy. This results in an increase in the discharged power to the grid from 40 kW to 44 kW. The additional injected power helps restore the frequency at point "C," which subsequently returns the discharged power to 40 kW.

On the other hand, during the charging process, the GESS enhances the power availability at the grid by decelerating the motor. This reduction in speed converts the kinetic energy of the rotating mass to potential energy and decreases the power drawn from the grid by the GESS from 40 kW to 36 kW. Consequently, the power available at the grid increases, assisting in the restoration of the frequency at point "C." Once the frequency is restored, the charging power reverts to 40 kW. Therefore, the GESS can effectively respond to frequency drops during both the charging and discharging phases, each with unique characteristics due to their opposing actions. Similarly, the GESS can also provide frequency regulation in the event of a frequency rise. Table II summarizes the operation of the GESS during the frequency regulation.

TABLE II. OPERATION OF GESS DURING FREQUENCY REGULATION.

Mode	Frequency	Speed	Active Power Injection/Absorption
Charging	$f > f_{rated}$	Increase	Increase absorption
	$f < f_{rated}$	Decrease	Decrease absorption
Discharging	$f > f_{rated}$	Decrease	Decrease injection
	$f < f_{rated}$	Increase	Increase injection

The amount of power exchanged during such contingencies is based on the extent of frequency variation and is limited by the power rating, energy capacity, and state of charge of the system. The duration of frequency regulation support and kinetic energy are constrained by the potential energy stored in the suspended mass, which is directly related to the system's storage capacity. This implies that the ability of the system to respond dynamically to grid frequency deviations is limited by the amount of potential energy stored in the mass. However, once the potential energy is fully utilized, the system's ability to support grid regulation diminishes, emphasizing the critical link with its storage capacity.

For instance, during discharge, if the frequency drops beyond 58.5 Hz, according to the frequency-watt curve, the power injection by the GESS should be 0.494 p.u. This suggests that a 40 kW rated system is expected to inject 59.76 kW, whereas a 30 kW rated system is expected to inject 44.82 kW of power. Similarly, the discharge duration is limited by the energy capacity and the state of charge of the system. A 40 kWh system with a state of charge at 100% will discharge for 40.16 minutes in response to the frequency drop below 58.5 Hz. However, if the state of charge is 50%, the length of discharge will reduce to 20.08 minutes.

B. Performance of a Low-Inertia Gravity Energy Storage System During Voltage Regulation

The GESS can provide reactive power compensation under voltage swell or swag based on the volt-VAR curve illustrated in Fig. 4. For the purpose of voltage regulation, the GESS primarily relies on the reactive power compensation. The reactive power compensation (Q) depends on the DC-link voltage (V_{DC}), grid voltage (V_{grid}), and boost inductor (L) as [26]

$$Q = 3V_{grid}\frac{V\cos\delta - V_{grid}}{\omega L} \tag{7-a}$$

$$V = \sqrt{\frac{3}{2}} m \frac{V_{DC}}{2} \tag{7-b}$$

where m is the modulation index, V is the converter input voltage, and δ is the power angle. Thus, for a constant DC-link voltage, the reactive power compensation is provided by regulating the converter input voltage and the power angle. Therefore, the reactive power compensation is independent of the kinetic energy of the rotating mass as well as the energy capacity of the GESS.

For example, Fig. 7 (a) shows an increase in grid voltage from a nominal 480 V at instant "A" to 510 V at instant "B." Prior to the voltage rise, the GESS is in the discharging mode delivering 3.5 kVAR to the grid due to the harmonic filter connected between the grid and the front-end converter. The reactive power injection remains constant until the voltage exceeds the deadband region at 494.4 V (1.03×480 V). As the voltage increases beyond 494.4 V and reaches 510 V, the GESS boosts the reactive power injection to 11.58 kVAR.

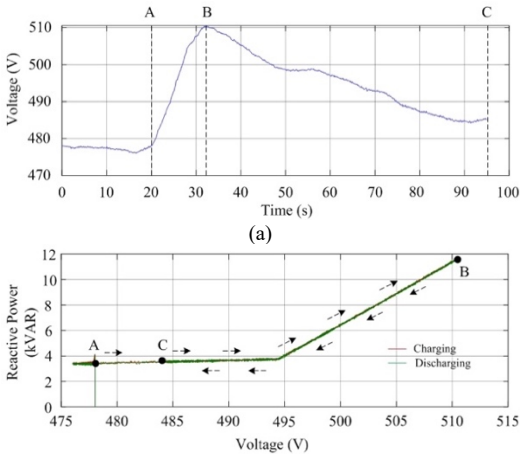

Fig. 7. Diagram of the voltage regulation to control the reactive power.

TABLE III. OPERATION OF GESS DURING VOLTAGE REGULATION.

Mode	Frequency	Speed	Reactive Power Injection/ Absorption
Charging	$V > V_{rated}$	No Change	Increase absorption
	$V < V_{rated}$	No Change	Decrease absorption
Discharging	$V > V_{rated}$	No Change	Increase injection
	$V < V_{rated}$	No Change	Decrease injection

This additional reactive power helps restore the voltage at instant "C," subsequently returning the reactive power to 3.5 kVAR. During this compensation, the reference reactive component of the grid current (igd*) is changed without changing the motor speed, and thus the active power supplied by or delivered to the grid remains unchanged. The responses of the GESS are the same, irrespective of the charging or discharging phase of the operation. Table III summarizes the operation of the GESS during voltage regulation.

C. *Impact of the GESS Electrical Machine Inertia on Frequency Regulation During Texas Grid Blackout*

As discussed earlier in equation (6), the kinetic energy (E_k) of the GESS in providing the frequency regulation support depends on the equivalent moment of inertia (J_{eq}) of the rotating masses and is expressed mathematically as

$$E_k = \frac{1}{2} J_{eq} \omega^2 = \frac{1}{2} (J_{rotor} + J_{mass}) \omega^2 \quad (8)$$

where, J_{rotor} represents the moment of inertia of the rotating mass, which comprises motor, winch, and sheave shaft, and J_{mass} represents the equivalent moment of inertia of the suspended mass. The equivalent rotor inertia (J_{rotor}) of the GESS, including winch and sheave, is expressed as

$$J_{rotor} = J_{motor} + \frac{J_{winch} + J_{sheave}}{N^2} \quad (9)$$

where $J_{machine}$, J_{winch}, and J_{sheave} are the moments of inertia of electrical machine, winch, and sheave, respectively, and N is the reduction ratio of the gearbox. The equivalent moment of inertia of suspended mass can be approximated from the net tension in the wire rope as

$$J_{mass} = \left(M_{cylinder} + M_{rope} - \frac{B}{g} \right) r^2 \quad (10)$$

where $M_{cylinder}$ is the mass of the cylinder, M_{rope} is the suspended mass of the rope by which the cylinder is suspended inside the well, B is the buoyant force acting on the cylinder and the rope, and r is the radius of the drum. The

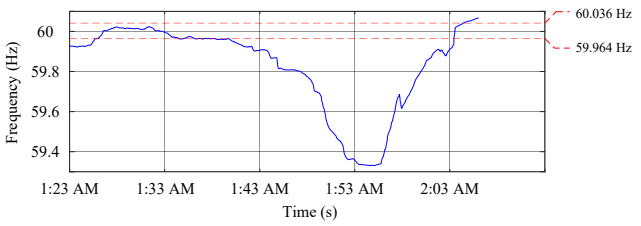

Fig. 8. The ERCOT grid frequency during load shedding and generation capacity outages on 15 February 2021 [23].

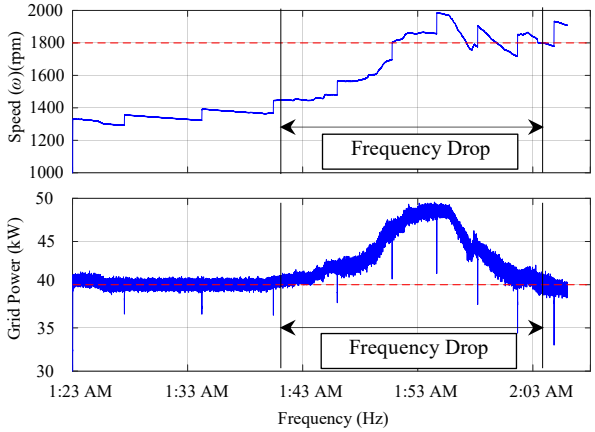

Fig. 9. The response of low-inertia machine-based GESS, showcasing the speed of the machine, and the active power injected to the grid under ERCOT grid frequency drop.

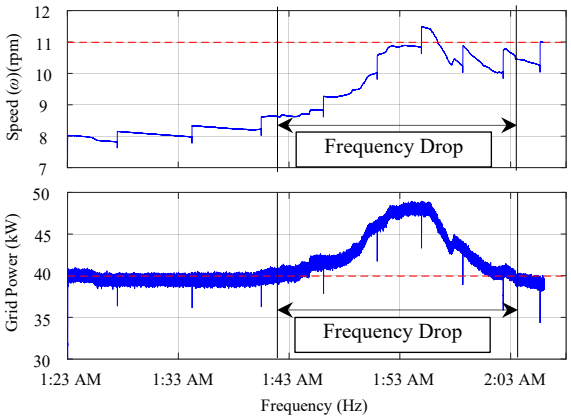

Fig. 10. The response of high-inertia machine-based GESS, showcasing the speed of the machine, and the active power injected to the grid under ERCOT grid frequency drop.

suspended mass of the rope and the radius varies with the position of the cylinder. Assuming that the weight of the cylinder and rope are held constant, it may be possible to increase the stored kinetic energy by increasing the equivalent moment of inertia of J_{rotor} by changing the drivetrain configuration from a geared system to a gearless system.

To study this impact we investigated the performance of two GESS with different equivalent rotor inertia assumed to be connected to the Texas grid. The previously developed GESS with low-inertia and high-speed motor was compared with a GESS with a high-inertia, low-speed direct-drive motor without using the gearbox. The direct-drive machine is a three-phase, 460 V, 11 rpm, 100 hp, permanent magnet synchronous machine with an inertia of 694.90 kg m^2.

However, the low-inertia machine-based GESS has an

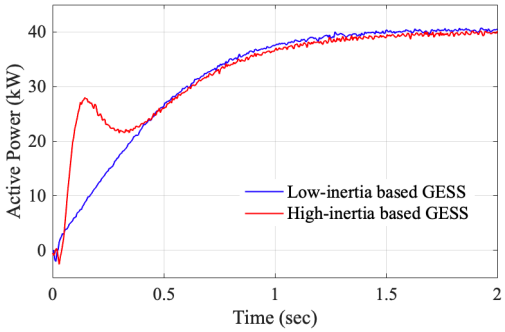

Fig. 11. Comparison between the response time of a low-inertia- and high-inertia-based GESS.

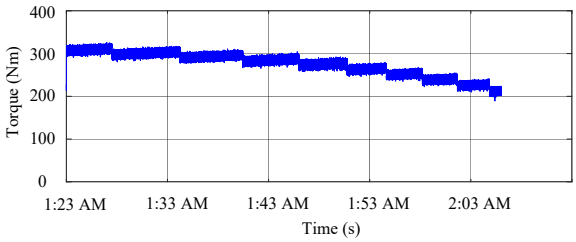

Fig. 12. The load torque at the machine shaft of the low-inertia GESS during ERCOT grid frequency drop .

inertia of 0.493 kg m^2. Considering a three-stage gearbox with a reduction ratio of 157.58, using equation (9), the equivalent rotor inertia of the low-inertia machine-based GESS is 0.2745 kg m^2, whereas the equivalent rotor inertia of the high-inertia machine-based GESS is 1407.14 kg m^2. The rest of the mechanical system is identical in both the systems, and therefore the equivalent moment of inertia of suspended mass of both the systems is the same.

We configured the controllers for both the GESS configurations and investigated their frequency regulation capabilities during an outage event that occurred in the Texas grid during on 15 February 2021 [23]. As shown in Fig. 8, the frequency dropped below 59.4 Hz due to load shedding and generation outage and lasts for 43 minutes.

The responses of the low-inertia and high-inertia machine-based GESS to the frequency drop when both systems were in discharging mode are illustrated in Fig. 9 and Fig. 10, respectively. Prior to the frequency drop, both the systems were discharging 40 kW to the grid.

Despite the differences in their inertia, responses to the frequency drop are similar. As illustrated in Fig. 11, both the systems deliver 40 kW rated power within 2 s, qualifying them for primary frequency response. Both the systems increase their active power injection when the frequency drops below the deadband region. When the frequency drops below 59.4 Hz, both the systems increased their power injection from 40 kW to 49 kW by increasing the discharge rate and accelerating the motor. For instance, the low-inertia machine accelerates from 1322 rpm to 1920 rpm to increase the power from 40 kW to 49 kW. Similarly, the speed of the high-inertia machine is increased from 8 rpm to 11.5 rpm, for the same increase in the power. Besides the frequency drop, the machine speed increases due to a layer change in the winch system. As the system discharges, the cylindrical mass is lowered into the well, causing the rope to unwind and reducing the effective radius of the winch system. Consequently, the load torque on

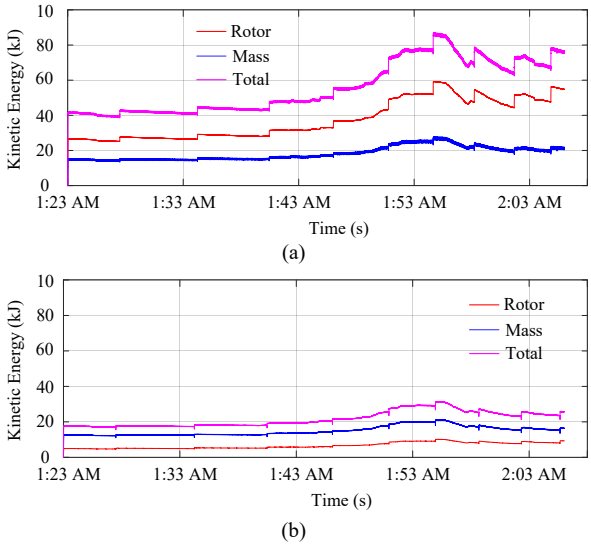

Fig. 13. Change in rotational kinetic energy during discharging; (a) low inertia, high speed motor system; (b) high inertia, direct-drive motor system.

the machine shaft decreases for the low-inertia motor, as shown in Fig. 12. To maintain constant power, the speed increases, causing the controller to invoke flux weakening to enable the motor to operate beyond its rated speed toward the conclusion of the discharge cycle. In the case of the high-inertia motor, the increase in speed is marginal, as its high inertia delivers the required energy with small variation in the speed. This is explained by the kinetic energy stored in the system, as illustrated in Fig. 13. The GESS with the low-inertia motor stores more maximum kinetic energy compared to the GESS with the high-inertia motor. This is due to the higher speed of the low-inertia system, which also affects the energy distribution. The GESS with the low-inertia motor requires a large change in kinetic energy to supply the same power to the grid, whereas the high-inertia system requires a relatively smaller change in kinetic energy. Since the frequency regulation support of the GESS is provided by the change in rotational speed, the system with the high-inertia motor will be able to provide the needed regulation over a longer or wider range of frequency variations, without significantly exceeding its rated speed. Conversely, the low-inertia system will entail flux-weakening, which can be detrimental to its lifetime. This can also be followed by comparing Fig. 8 and Fig. 9, where the low-inertia system spends a longer time beyond rated speed compared to the high-inertia system.

Both systems delivered 30 kWh of energy during the discharge operation. Of this total, 27.18 kWh came from constant discharge, while the remaining 2.83 kWh was supplied in response to the frequency drop. This implies that, if the system state of charge is below 30 kWh, both systems may not be able to support the grid for the entire duration of the frequency drop. Thus, the frequency regulation capability of the GESS is contingent on the duration of frequency variation and is limited by the power rating and state of charge of the GESS. The duration of frequency regulation support and kinetic energy are constrained by the potential energy stored in the suspended mass, which is directly related to the system's storage capacity. This implies that the ability of the system to respond dynamically to grid frequency deviations is limited by the amount of potential energy stored in the mass.

VI. Conclusion

In this study, the frequency and voltage regulation capabilities of GESS were studied. A MATLAB-based model of the GESS was developed, and the control algorithms for frequency and voltage regulation were introduced.

The results indicated that the response time of the GESS with frequency and voltage regulation is within 2 s, demonstrating its capability to provide primary frequency response. Unlike the results reported in previous studies [22], the present work showed that the GESS can provide frequency regulation support during both modes of operation, i.e., charging and discharging. This is possible by increasing the power availability on the grid by accelerating the motor during charging and decelerating the motor during discharging. Because the GESS relies on a DC-link decoupled inverter-drive system, voltage regulation support is possible by reactive power injection from the grid without altering the motor speeds during charging or discharging mode.

The frequency regulation capabilities of two different GESS with a low- and high-inertia motor were demonstrated to be similar during a Texas electric grid blackout event in 2021. However, because frequency regulation relies on the change in rotational speed, the high-inertia system may be able to operate over a broader range of frequency variations without exceeding its rated speed. In contrast, a low-inertia system requires flux-weakening, which can negatively impact its lifespan.

The frequency regulation capability of a GESS is also contingent on the duration of frequency variation, and it is limited by the power rating and state of charge of the GESS.

References

[1] ERCOT Nodal Operating Guide, [Online] https://www.ercot.com/files/docs/2021/12/21/Nodal%20Operating%20Guide.pdf, Accessed on: 17 July 2024.

[2] L. Meng *et al*., "Fast frequency response from energy storage systems—A review of grid standards, projects and technical issues," *IEEE Trans. on Smart Grid*, vol. 11, no. 2, pp. 1566-1581, March 2020, doi: 10.1109/TSG.2019.2940173.

[3] E. Lannoye, D. Flynn and M. O'Malley, "The role of power system flexibility in generation planning," in *Proc.IE EE Power and Energy Society General Meeting*, Detroit, MI, USA, pp. 1-6, 2011.

[4] Y. -K. Wu, W. -S. Tan, S. -R. Huang, Y. -S. Chiang, C. -P. Chiu and C. -L. Su, "Impact of generation flexibility on the operating costs of the taiwan power system under a high penetration of renewable power," *IEEE Trans. Ind. Appl.*, vol. 56, no. 3, pp. 2348-2359, May-June 2020.

[5] J. Mays, "Generator interconnection, network expansion, and energy transition," *IEEE Trans. Energy Markets, Policy and Regulation*, vol. 1, no. 4, pp. 410-419, Dec. 2023.

[6] S. -Y. Su, C. -N. Lu, R. -F. Chang and G. Gutiérrez-Alcaraz, "Distributed generation interconnection planning: A wind power case study," *IEEE Trans. Smart Grid*, vol. 2, no. 1, pp. 181-189, March 2011.

[7] H. García-Pereira, M. Blanco, G. Martínez-Lucas, J. I. Pérez-Díaz and J. -I. Sarasúa, "Comparison and influence of flywheels energy storage system control schemes in the frequency regulation of isolated power systems," *IEEE Access*, vol. 10, pp. 37892-37911, 2022.

[8] J. Yu, J. Fang and Y. Tang, "Inertia emulation by flywheel energy storage system for improved frequency regulation," in *Proc. IEEE 4th Southern Power Electron. Conf. (SPEC)*, Singapore, pp. 1-8, 2018.

[9] M. Rouholamini *et al*., "A review of modeling, management, and applications of grid-connected Li-Ion battery storage systems," *IEEE Trans. Smart Grid*, vol. 13, no. 6, pp. 4505-4524, Nov. 2022,

[10] Y. Shi, B. Xu, D. Wang and B. Zhang, "Using battery storage for peak shaving and frequency regulation: Joint optimization for superlinear gains," *IEEE Trans. Power Sys.*, vol. 33, no. 3, pp. 2882-2894, May 2018.

[11] J. Fang, H. Li, Y. Tang and F. Blaabjerg, "On the inertia of future more-electronics power systems," *IEEE Trans. Emerg. Sel. Topics Power Electron.*, vol. 7, no. 4, pp. 2130-2146, Dec. 2019.

[12] S. Sahoo and P. Timmann, "Energy storage technologies for modern power systems: A detailed analysis of functionalities, potentials, and impacts," *IEEE Access*, vol. 11, pp. 49689-49729, 2023.

[13] S. Karpana, E. I. Batzelis, G. Kampitsis, S. Maiti and C. Chakraborty, "A soft-switched multi-port converter for PV/Supercapacitors hybrid systems enabling frequency response services," *IEEE Trans. Ind. Appl.*, vol. 60, no. 3, pp. 4541-4556, May-June 2024.

[14] A. G. Papakonstantinou, A. I. Konstanteas and S. A. Papathanassiou, "Solutions to enhance frequency regulation in an island system with pumped-hydro storage under 100% renewable energy penetration," *IEEE Access*, vol. 11, pp. 76675-76690, 2023.

[15] Y. Chen, W. Xu, Y. Liu, Z. Bao, Z. Mao and E. M. Rashad, "Modeling and transient response analysis of doubly-fed variable speed pumped storage unit in pumping mode," *IEEE Trans. Ind. Electron.*, vol. 70, no. 10, pp. 9935-9947, Oct. 2023.

[16] L. Shi, W. Lao, F. Wu, T. Zheng and K. Y. Lee, "Frequency regulation control and parameter optimization of doubly-fed induction machine pumped storage hydro unit," *IEEE Access*, vol. 10, pp. 102586-102598, 2022.

[17] C. D. Botha, M.J. Kamper, "Capability study of dry gravity energy storage", *J. Energy Storage*, Vol. 23, pp. 159-174, 2019.

[18] Q. Wang, Y. Li, Q. Zhang, D. He and D. Wang, "Fast voltage regulation and grid connection method for generator-motor of vertical gravity energy storage systems," *in Proc. Int. Conf. Clean Energy Storage Power Engg. (CESPE)*, Xi'an, China, pp. 31-32, 2023.

[19] T. Dragičević, X. Lu, J. C. Vasquez and J. M. Guerrero, "DC microgrids - Part II: A review of power architectures, applications, and standardization issues," *IEEE Trans. Power Electron.*, vol. 31, no. 5, pp. 3528-3549, May 2016, doi: 10.1109/TPEL.2015.2464277.

[20] Inertia: Basic concepts and impacts on the ERCOT grid, ERCOT, [Online] https://www.ercot.com/files/docs/2018/04/04/Inertia_Basic_Concepts_Impacts_On_ERCOT_v0.pdf, Accessed on: 22 June 2024.

[21] Gravitircity, [Online] https://gravitricity.com/technology/, Accessed on: 17 July 2024.

[22] W. Tong, Z. Lu, M. Han, H. Zhao, G. Xu, G. Zhao, J. D. Hunt, "Inertial characteristics of gravity energy storage systems," *preprint, ResearchGate,* Nov. 2023, To be published.

[23] P.V., Jaquez Converting oil and gas wells to energy storage, Renewell, [Online] https://renewellenergy.com/wp-content/uploads/2022/11/P1-Converting-Wells-to-Energy-Storage-Renewell-Energy-1.pdf, Accessed on 22 June 2024.

[24] Energy institute, The university of Texas, Austin, The timeline and events of the february 2021 Texas electric grid blackouts, [Online] https://energy.utexas.edu/sites/default/files/UTAustin%20%282021%29%20EventsFebruary2021TexasBlackout%2020210714.pdf, Accessed on: 22 June 2024.

[25] Baldor Reliance Motors, [Online] https://www.baldor.com/catalog/ZDPM25100-BV#tab=%22specs%22, Accessed on: 22 June 2024.

[26] Siva Prasad, J.S., Bhavsar, T., Ghosh, R. et al. "Vector control of three-phase AC/DC front-end converter", *Sadhana*, 33, pp. 591–613, May 2009.